Joint Spatial and Propagation Models for Cellular Networks

Anjin Guo and Martin Haenggi
Department of Electrical Engineering
University of Notre Dame
Notre Dame, IN, USA
E-mail: {aguo, mhaenggi}@nd.edu

***Abstract*—In all current models for cellular networks, independent randomness in the positions of the base stations (BSs) and the propagation conditions is assumed. In practice, however, in coverage-oriented deployments, where the goal is to achieve good baseline coverage, cellular operators place the base stations further apart if propagation is favorable, and vice versa. We thus propose a new class of cellular model, where BSs are deployed such that all cell edge users achieve a minimum target signal power level from the serving BS. The spatial structure of the BSs is a result of the propagation environment and the target signal power. We call such network models joint spatial and propagation (JSP) models. To formulate such models, we assume the path loss follows a power law with a variable path loss exponent, so that the target signal power is achieved at the cell edges, given the distribution of the BSs. The coverage probability, defined as the probability that the signal-to-interference-plus-noise-ratio (SINR) exceeds a threshold, is evaluated and compared with the standard Poisson and lattice models. Our results show that networks with Poisson distributed BSs appear to the user like lattice networks if the dependence between BS placement and propagation is accounted for.**

I. Introduction

In all current models for cellular networks, independent randomness in the positions of the base stations (BSs) and the propagation models (path loss and fading) is assumed, e.g., [1]–[6]. In [1], the authors assumed a homogeneous Poisson distributed network and the power-law path loss model $\ell(x) = \|x\|^{-\alpha}$, where $x \in \mathbb{R}^2$ and calculated the coverage probability, defined as the complementary cumulative distribution function (CCDF) of the SINR, i.e., $P_{\mathrm{c}}(\theta) = \mathbb{P}(\mathrm{SINR} > \theta)$. Under the assumptions of Rayleigh fading, no noise and $\alpha = 4$, $P_{\mathrm{c}}(1) = 0.56$ and $P_{\mathrm{c}}(10) = 0.20$. The main reason why the result is so pessimistic is that mobile users near the edge suffer from low signal strength in large cells. In [2], the authors used the β-Ginibre point process, where points exhibit repulsion, to model the spatial distribution of the BSs and considered the bounded power-law path loss model $\ell(r) = (\max\{r_0, r\})^{-\alpha}$, where r_0 is a positive constant and $r \in \mathbb{R}^+$. The coverage probability is better than that of the Poisson network, since in the β-Ginibre network ($\beta > 0$), BSs are less likely to be close to each other and thus severe interference from nearby BSs is avoided. Moreover, the variance of the cell size is reduced.

In practice, when the goal of the BS deployment is to achieve good baseline coverage, cellular operators place the BSs further apart if propagation is favorable, and vice versa. Thus, a large cell implies smaller path loss or less severe shadowing, and vice versa. This dependence between cell sizes and propagation has been completely ignored, despite (as we shall see) having a significant impact on the performance analysis. In large cells, users near cell edges usually suffer from unsatisfactory communication conditions with low received signal power, in addition to being subject to relatively high interference. In reality, to avoid those bad situations, cellular operators would place another BS to reduce the cell size and improve the signal strength of edge users. The optimal situation would be that the received signal strengths along all cell edges are equal and meet the minimum requirement.

In this paper, we propose a new class of cellular models, where all users at the cell edges achieve a minimum target signal power level from their serving BSs. The spatial structure of the BSs is a result of the propagation environment and the target signal power. We call such models joint spatial and propagation (JSP) models. One special case of the JSP model is the triangular lattice (which has hexagonal cells) with independent power-law path loss model, where the received signal power at the cell edges is approximately the same.

In this paper, to formulate JSP models, we assume the path loss still follows the power law, but the path loss exponent is variable to satisfy the requirement of the target signal power at the cell edges, given a distribution of the BSs. We derive the coverage probability analytically and obtain simulation results. To our best knowledge, this is the first work that takes into account the dependence between cell sizes and shapes and signal propagation.

II. System Model

We introduce a novel cellular downlink model, where all BSs are always transmitting with equal power P and are *well* deployed, which means that the signal power averaged over the fading from each BS at its *cell edge* is always equal to a constant target received power $P_0 < P$, as is illustrated in Fig. 1. The cell edge is defined as the association boundary for mobile users, inside which at any location, the received signal power averaged over the fading from the BS in the cell is larger than the signal power from any other BS. We assume the frequency reuse factor is 1. Thus all other BSs act as interferers. All signals are assumed to experience path loss

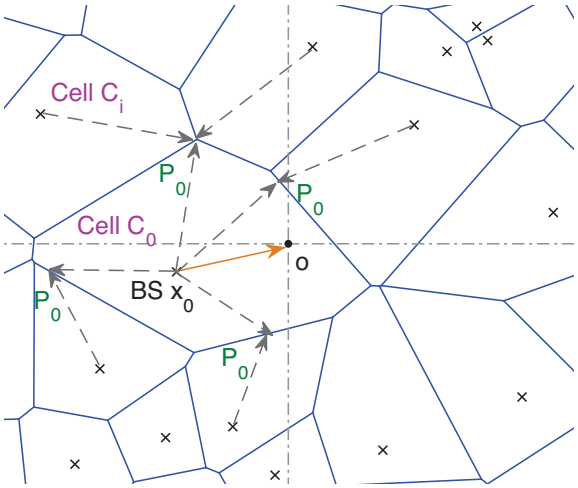

Fig. 1. BSs (denoted by '×') and cell edges (e.g., the Voronoi tessellation). For any point on the cell edges, the received signal power averaged over the fading from any one of the closest two or three BSs is a constant P_0.

and independent (small-scale) Rayleigh fading with mean 1. Without loss of generality, in our model, we assume $P = 1$.

Due to the factors such as terrain contours, environment (urban or rural, vegetation and foliage), propagation medium, etc., which influence the path loss of a signal, the cell shape in real networks and in our model is not hexagonal but irregular. From a global perspective, the BSs appear to be deployed randomly and thus may be modeled as a homogenous Poisson point process (PPP) or some non-Poisson point process, such as the Ginibre process. In the rest of the paper, we assume that the BSs follows a homogeneous PPP with intensity λ.

The path loss in our model is not modeled as the conventional one, i.e., a power law path loss model with a fixed path loss exponent. Instead, we consider the power law path loss model from x to the origin o as $\ell(x) = \|x\|^{-\alpha}$, where α is variable. The path loss exponent α is affected by the aforementioned factors and some other factors such as refraction, diffraction, reflection and absorption. Therefore, it is α that determines the shape of a cell. For simplicity, we assume in a cell C_i, the path loss exponent is a function of the direction ω from the BS, denoted by $\alpha_i(\omega)$. We call this path loss exponent *local path loss exponent*.

III. Poisson Networks and Voronoi Tessellations

The BS placement and the cell edges are a function of the propagation environment. Assuming that the resulting deployment is a PPP, we can *reverse engineer* the local path loss exponents α if the cell edges are known. We assume the cells correspond to the Poisson-Voronoi tessellation, which means that the serving BS of a mobile user is the one closest to the user. An illustration of our system model is shown in Fig. 1. Given a specific deployment of BSs on the plane, the cell edges are known from the Voronoi tessellation, and $\alpha_i(\omega)$ in each cell C_i can then be calculated.

In this section, we mainly analyze the *coverage probability*, defined as the CCDF of the signal-to-interference-plus-noise ratio (SINR), i.e., $P_c(\theta) \triangleq \mathbb{P}(\text{SINR} > \theta)$. We consider a typical user at the origin o, as is shown in Fig. 1, and denote the cell that contains o as C_0 and its size as S_0.

The interference to the typical user is the accumulated signal power from all BSs other than the serving BS. Analyzing the interference is difficult for two reasons:

1) In the Poisson-Voronoi tessellation, conditioned on the Voronoi cell C_0 containing o, the locations of the interfering BSs in the adjacent Voronoi cells are determined, which means the received signal power is correlated with the interference. But such correlation is not necessarily difficult to deal with since we know we can handle it with the standard path loss model. It is only together with the dependent propagation model that this becomes difficult. To tackle the problem, in the rest of this paper, we approximate irregular cell shapes as disks[1] of the same cell size and we make assumptions that the serving BS at x_0 is still the closest BS to the origin (regardless of the shape of the cell in the approximation we have made—"disk") and the interfering BSs follow a PPP with intensity λ outside the disk $b(o, \|x_0\|)$.
2) In the Poisson-Voronoi tessellation, it is hard to analyze the path loss that the interfering signal from an interfering BS experiences. The path loss depends on the path the signal traverses, and the local path loss exponents vary from cell to cell and also depend on the direction, which makes an exact calculation of the path loss intractable. To simplify the analysis, we assume that all interfering signals experience a path loss with a fixed path loss exponent $\bar{\alpha}$.

A. Cell Shape: Irregular Shape and Disk

Consider the Voronoi cell C_i and assume the BS of C_i is at the origin, as is shown in Fig. 2. B_i is disk First, we make some comparisons between the actual shape of C_i and the disk B_i with the same size.

1) Distribution of the Desired Signal Power Averaged over the Fading: For a mobile user at x in C_i, the received signal power averaged over the fading, denoted as $P_r(x)$, is expressed as $P_r(x) = \|x\|^{-\alpha_i(\angle x)}$, which depends on the distance to the origin $\|x\|$ and the corresponding local path loss exponent $\alpha_i(\angle x)$, where $\angle x$ the angle from the serving BS to x.

For a mobile user who is uniformly distributed in the cell, the cumulative distribution function (CDF) of the desired signal power $\hat{P}_r$ averaged over the fading is denoted by $F_{\hat{P}_r}(y) = \mathbb{P}(\hat{P}_r < y)$, where $y \geq P_0$. In the rest of this subsection, we compare the CCDF of the desired signal power averaged over the fading in the Voronoi cell C_i of size $S_i = S > 0$ with that in B_i.

As is illustrated in Fig. 2, denote by $r(\omega)$ the distance from the BS to its Voronoi cell edge with angle ω. It follows that $S = \frac{1}{2}\int_0^{2\pi} (r(\omega)^2) dw$. Since $r(\omega)^{-\alpha_i(\omega)} = P_0$, we have

[1] In [7], it has been proved that asymptotically, large cells are indeed disks. So the disk assumption makes sense at least when cell size is large. In Section IV, we will show by simulations that the approximation is good.

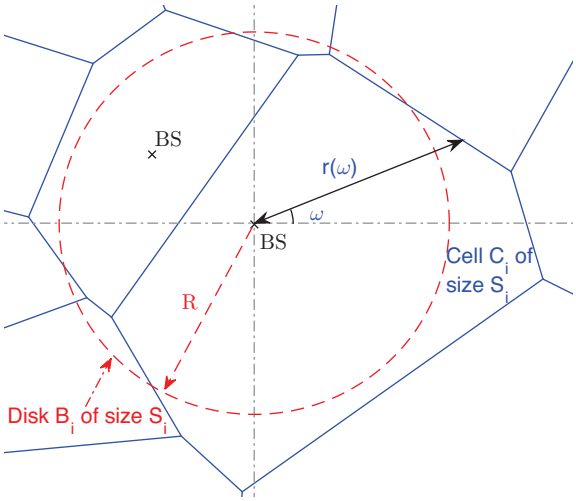

Fig. 2. The Voronoi cell C_i of size $S_i = S$ and its corresponding disk B_i of the same size. $r(\omega)$ is the distance from the BS to its cell edge with angle ω. $R = \sqrt{\frac{S}{\pi}}$ is the radius of B_i.

$\alpha_i(\omega) = -\frac{\ln P_0}{\ln r(\omega)}$. We have $\alpha_i(\omega) < 0$ if $r(\omega) < 1$, and $\alpha_i(\omega) > 0$ if $r(\omega) > 1$. Therefore, for $1 \geq y \geq P_0$,

$$\begin{aligned} F^c_{P_r}(y) &= \mathbb{P}(P_r > y) = \mathbb{E}_{x\in C_i}[\mathbf{1}(\|x\|^{-\alpha_i(\angle x)} > y)] \\ &= \frac{1}{S}\int_0^{2\pi}\int_0^{y^{-\frac{1}{\alpha_i(\omega)}}} \mathbf{1}(r(\omega) > 1) z dz dw \\ &= \frac{1}{2S}\int_0^{2\pi} y^{-\frac{2}{\alpha_i(\omega)}}\mathbf{1}(r(\omega) > 1) dw \\ &= \frac{1}{2S}\int_0^{2\pi} (r(\omega)^2)^{\frac{\ln y}{\ln P_0}}\mathbf{1}(r(\omega) > 1) dw. \end{aligned} \quad (1)$$

In disk B_i of size S with radius $R = \sqrt{\frac{S}{\pi}}$, to meet the assumption of equal power at the cell edge, the local path loss exponent α is the same everywhere in B_i, and we have $R^{-\alpha} = P_0$. So, $\alpha = -\frac{2\ln P_0}{\ln S - \ln \pi}$.

For $S > \pi$, we have $\alpha > 0$ and $R > 1$. The CCDF of the desired signal power $\tilde{P}_r$ averaged over the fading in B_i, denoted as $F^c_{\tilde{P}_r}$, is

$$\begin{aligned} F^c_{\tilde{P}_r}(y) &= \mathbb{P}(\tilde{P}_r > y) = \mathbb{E}_{x\in b(o,R)}[\mathbf{1}(\|x\|^{-\alpha} > y)] \\ &= \frac{1}{S}\int_0^{2\pi}\int_0^{y^{-\frac{1}{\alpha}}} z dz dw \\ &= \frac{1}{S}\pi y^{-\frac{2}{\alpha}} = \frac{\pi}{S}\left(\frac{S}{\pi}\right)^{\frac{\ln y}{\ln P_0}}. \end{aligned} \quad (2)$$

Since $1 \geq y \geq P_0$, $H(x) = x^{\frac{\ln y}{\ln P_0}}$ is a concave function for $x > 0$. By Jensen's inequality, we have

$$\begin{aligned} F^c_{\tilde{P}_r}(y) &= \frac{\pi}{S}\frac{1}{2\pi}\int_0^{2\pi} (r(\omega)^2)^{\frac{\ln y}{\ln P_0}}\mathbf{1}(r(\omega) > 1) dw \\ &\leq \frac{\pi}{S}\frac{1}{2\pi}\int_0^{2\pi} (r(\omega)^2)^{\frac{\ln y}{\ln P_0}} dw \\ &\leq \frac{\pi}{S}\left(\frac{1}{2\pi}\int_0^{2\pi} (r(\omega)^2) dw\right)^{\frac{\ln y}{\ln P_0}} \\ &= \frac{\pi}{S}\left(\frac{S}{\pi}\right)^{\frac{\ln y}{\ln P_0}} = F^c_{\hat{P}_r}(y). \end{aligned} \quad (3)$$

According to (3), $\tilde{P}_r$ in B_i stochastically dominates $\hat{P}_r$ in C_i. In the rest of the paper, we approximate the cell shape with a disk of the same size. In doing so, for cell size $S > \pi$, the CCDF of the desired signal power averaged over the fading becomes larger and thus, the average received signal power P_r over the whole cell $\frac{1}{|C_i|}\int_{x\in C_i} P_r(x)dx$ becomes larger.

For $S < \pi$, we have $\alpha < 0$, $R < 1$ and $F^c_{\tilde{P}_r}(y) = \mathbb{E}_{x\in b(o,R)}[\mathbf{1}(\|x\|^{-\alpha} > y)] = 0$. Thus, $F^c_{\hat{P}_r}(y) \geq F^c_{\tilde{P}_r}(y)$. $\hat{P}_r$ in C_i stochastically dominates $\tilde{P}_r$ in B_i. When the intensity of the PPP becomes small, the case of $S < \pi$ can be ignored.

2) Distribution of the distance from a user to the BS: For a user who is uniformly distributed in C_i, denote the CDF of the distance from it to the BS $\hat{d}$ as $F_{\hat{d}}$. For a user who is uniformly distributed in the disk B_i with the same size as C_i, denote the CDF of the distance from it to the BS $\tilde{d}$ as $F_{\tilde{d}}$. It is obvious that $F_{\tilde{d}}(x) \geq F_{\hat{d}}(x)$, for all $x \geq 0$. $\tilde{d}$ in B_i stochastically dominates $\hat{d}$ in C_i. Therefore, with the approximation, the mean distance from a user to the BS becomes smaller.

B. Coverage Analysis

As is mentioned in Section III-A, we assume all Voronoi cells can be treated as disks. In [8], it has been derived that the *normalized* probability density function (PDF) of the Voronoi cell sizes in the plane can be approximated as

$$f_{\bar{S}}(x) = \frac{c^c}{\Gamma(c)}x^{c-1}\exp(-cx), \quad (4)$$

where $c = \frac{7}{2}$ and $\bar{S} = \lambda S$ is the normalized cell size. (The mean of Voronoi cell size S for any stationary point process with intensity λ is $\frac{1}{\lambda}$.) Thus, the Voronoi cell size S for a PPP with intensity λ follows the gamma distribution with parameters c and $\frac{1}{\lambda c}$, denoted as gamma$(c, \frac{1}{\lambda c})$, and the PDF of S is

$$f_S(x) = \frac{(\lambda c)^c}{\Gamma(c)}x^{c-1}\exp(-\lambda c x). \quad (5)$$

For the typical user at o with serving cell size S_0, conditioned on S_0, the serving BS is uniformly distributed on the disk B_0 of size S_0, and thus the CDF of the distance d from the BS to the origin is $\hat{F}_d(x) = \frac{\pi}{S_0}x^2$, for $0 \leq x \leq \sqrt{\frac{S_0}{\pi}}$. Therefore, conditioning on the serving cell size S_0 and the serving BS at x_0, which is subject to $S_0 > \pi x_0^2$, we have the desired received power at the origin o

$$P_r = h_0\|x_0\|^{-\alpha_0}, \quad (6)$$

where h_0 is the fading parameter satisfying $h_0 \sim \text{Exp}(1)$ and $\alpha_0 = -\frac{2\ln P_0}{\ln S_0 - \ln \pi}$. The interference can be expressed as

$$I_{x_0} = \sum_{x\in\Phi\setminus b(o,\|x_0\|)} h_x\|x\|^{-\bar{\alpha}}, \quad (7)$$

where $\{h_x\}$ are the i.i.d. fading parameters that follow Exp(1) and are independent of h_0. Assume the thermal noise is additive and constant with power W. This gives the SINR expression

$$\text{SINR} = \frac{h_0\|x_0\|^{-\alpha_0}}{\sum_{x\in\Phi\setminus b(o,\|x_0\|)} h_x\|x\|^{-\bar{\alpha}} + W}. \tag{8}$$

In this section, for the interfering signal, we assume the fixed path loss exponent $\bar{\alpha}$ is the average of the local path loss exponent (under the disk approximation) over the plane, which is given as

$$\bar{\alpha} = \frac{\int_0^\infty \alpha_x x f_S(x)dx}{\int_0^\infty x f_S(x)dx}, \tag{9}$$

where $\alpha_x \triangleq -\frac{2\ln P_0}{\ln x - \ln \pi}$. However, by the properties of the logarithmic integral function, we have $\int_0^\pi \alpha_x dx = -\infty$ and $\int_\pi^\zeta \alpha_x dx = +\infty$ for any $\pi < \zeta < \infty$. To avoid considering the singularity of α_x, we choose a constant $\tau_0 > \pi$ and define $\bar{\alpha}$ as

$$\begin{aligned}\bar{\alpha} &= \frac{\int_{\tau_0}^\infty \alpha_x x f_S(x)dx + \int_0^{\tau_0} \alpha_{\tau_0} x f_S(x)dx}{\int_0^\infty x f_S(x)dx} \\ &= \int_0^\infty \frac{-2\ln P_0}{\ln(\max\{x,\tau_0\}) - \ln\pi} \frac{(\lambda c)^{c+1}}{\Gamma(c+1)} x^c \exp(-\lambda c x)dx,\end{aligned} \tag{10}$$

where $\alpha_{\tau_0} \triangleq -\frac{2\ln P_0}{\ln \tau_0 - \ln \pi}$. In the rest of the paper, we set $\tau_0 = 4$. The coverage probability is given in the following theorem.

Theorem 1. *In the JSP model consisting of disk-shaped cells whose sizes follow gamma$(c, \frac{1}{\lambda c})$, the coverage probability is*

$$\begin{aligned}P_{\mathrm{c}}(\theta) = \int_0^\infty \frac{2\pi}{v} \int_0^{\sqrt{\frac{v}{\pi}}} \exp\Big(- y^{\alpha_v}\theta W - 2\pi\lambda \\ \cdot \int_y^\infty \Big(1 - \frac{1}{1 + y^{\alpha_v}\theta z^{-\bar{\alpha}}}\Big) z dz\Big) y dy f_{S_0}(v)dv,\end{aligned} \tag{11}$$

where $\alpha_x \triangleq -\frac{2\ln P_0}{\ln x - \ln \pi}$, $f_{S_0}(x) = \frac{(\lambda c)^{c+1}}{\Gamma(c+1)} x^c \exp(-\lambda c x)$ and $\bar{\alpha}$ is expressed in (10)*.*

Proof: Let us first derive the CDF $F_{S_0}(x)$ of the size S_0 of the cell that contains o. Since the probability of o falling into a cell with size smaller than x is equal to the area ratio of all cells with size smaller than x to the entire plane, we have

$$\begin{aligned}F_{S_0}(x) = \mathbb{P}(S_0 < x) &= \frac{\int_0^x z \frac{(\lambda c)^c}{\Gamma(c)} z^{c-1}\exp(-\lambda c z)dz}{\int_0^\infty z \frac{(\lambda c)^c}{\Gamma(c)} z^{c-1}\exp(-\lambda c z)dz} \\ &= \lambda \int_0^x \frac{(\lambda c)^c}{\Gamma(c)} z^c \exp(-\lambda c z)dz.\end{aligned} \tag{12}$$

(12) is shown in a more general context in [9]. The PDF of S_0 is thus $f_{S_0}(x) = \frac{(\lambda c)^{c+1}}{\Gamma(c+1)} x^c \exp(-\lambda c x)$. So, $S_0 \sim$ gamma$(c+1, \frac{1}{\lambda c})$.

The coverage probability can be expressed as

$$\begin{aligned}P_{\mathrm{c}}(\theta) &= \mathbb{P}(\text{SINR} > \theta) \\ &= \int_0^\infty \mathbb{P}(\text{SINR} > \theta \mid S_0 = v) f_{S_0}(v)dv.\end{aligned} \tag{13}$$

Conditioning on $S_0 = v$, we have the coverage probability in the following form.

$$\begin{aligned}&\mathbb{P}(\text{SINR} > \theta \mid S_0 = v) = \mathbb{E}_{x_0}\mathbb{P}\left(\frac{h_0\|x_0\|^{-\alpha_v}}{I_{x_0} + W} > \theta \mid x_0\right) \\ &= \mathbb{E}_{x_0}\mathbb{E}_{I_{x_0}}\big(\exp(-\|x_0\|^{\alpha_v}\theta(I_{x_0} + W))\big) \\ &= \int_0^{\sqrt{\frac{v}{\pi}}} \exp(-y^{\alpha_v}\theta W)\mathbb{E}_{I_y}\big(\exp(-y^{\alpha_v}\theta I_y)\big)\hat{f}_d(y)dy,\end{aligned} \tag{14}$$

where $\hat{f}_d(y) = \frac{2\pi}{S_0} y$, for $0 \le y \le \sqrt{\frac{S_0}{\pi}}$ is the PDF of the distance d from the serving BS to the origin, $\alpha_x \triangleq -\frac{2\ln P_0}{\ln x - \ln \pi}$ and $I_y = \sum_{x\in\Phi\setminus b(o,y)} h_x\|x\|^{-\bar{\alpha}}$. Since the Laplace transform of I_y is

$$\begin{aligned}\mathcal{L}_{I_y}(s) &= \mathbb{E}_{I_y}(\exp(-sI_y)) \\ &= \mathbb{E}\Big(\exp\Big(-s\sum_{x\in\Phi\setminus b(o,y)} h_x\|x\|^{-\bar{\alpha}}\Big)\Big) \\ &= \exp\Big(-2\pi\lambda\int_y^\infty \Big(1 - \frac{1}{1+sz^{-\bar{\alpha}}}\Big) z dz\Big),\end{aligned} \tag{15}$$

combining (14) and (15) yields that

$$\begin{aligned}&\mathbb{P}(\text{SINR} > \theta \mid S_0 = v) \\ &= \frac{2\pi}{v}\int_0^{\sqrt{\frac{v}{\pi}}} \exp\Big(-y^{\alpha_v}\theta W \\ &\quad - 2\pi\lambda\int_y^\infty \Big(1 - \frac{1}{1 + y^{\alpha_v}\theta z^{-\bar{\alpha}}}\Big) z dz\Big) y dy.\end{aligned} \tag{16}$$

Combining (13) and (16), we obtain (11). ∎

IV. Simulations

We have analyzed the JSP model in Poisson networks by approximating irregular cell shapes as disks. In this section, we first investigate whether such approximation has good accuracy by comparing the approximation results with the simulation results of the JSP model with irregular cell shapes. Then, the distribution of the local path loss exponent is investigated. Finally, we make a comparison between our JSP model and the *conventional* models, where the path loss exponent is a constant and the desired received signal power averaged over the fading at cell edges is not a constant [1], [3].

As is discussed in Section III-A, for any user at x in the Voronoi cell C_i in the JSP model with irregular cell shapes, the local path loss exponent $\alpha_i(\angle x)$ for the desired received signal is determined by the angle from the serving BS to x and the cell shape, i.e. $\alpha_i(\angle x) = -\frac{\ln P_0}{\ln r(\angle x)}$. For all interfering signals from other BSs, we assume the path loss exponent is constant and given in (10).

The simulations are performed on a 4000×4000 square. We take, unless otherwise specified, the intensity of the PPP $\lambda = 3.5 \times 10^{-5}$, which is reasonable if the distance unit is meter, since it is close to the density of BSs in one typical urban region in the UK (see [4] for details). We set $P_0 = 1 \times 10^{-8}$ unless otherwise specified. If the power unit is Watt,

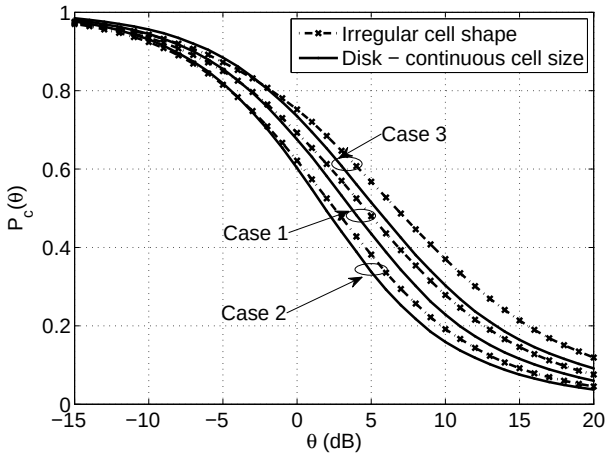

Fig. 3. The coverage probability $P_{\rm c}(\theta)$ vs. θ for the JSP model with irregular cell shapes and disk approximation of the cell shape in three parameter setting cases. Case 1: $\lambda = 3.5 \times 10^{-5}, P_0 = 1 \times 10^{-8}, \bar{\alpha} = 4.0$; Case 2: $\lambda = 3.5 \times 10^{-5}, P_0 = 1 \times 10^{-7}, \bar{\alpha} = 3.5$; Case 3: $\lambda = 1 \times 10^{-4}, P_0 = 1 \times 10^{-8}, \bar{\alpha} = 4.5$.

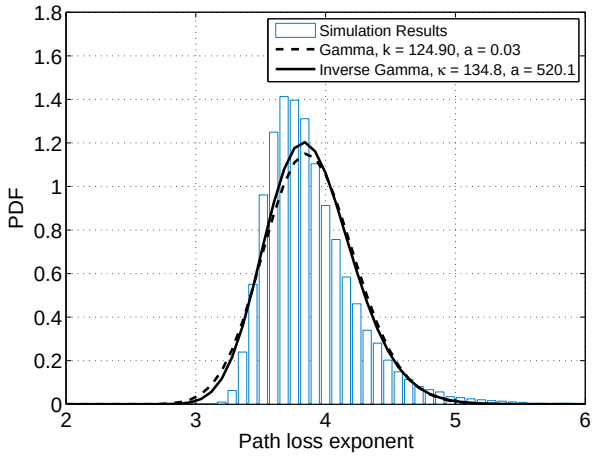

Fig. 4. Empirical PDF of the local path loss exponent for the desired received signal and the fits of the gamma distribution and the inverse gamma distribution ($\lambda = 3.5 \times 10^{-5}$, $P_0 = 1 \times 10^{-8}$ and $\bar{\alpha} = 4.0$). The average of the empirical local path loss exponents is 3.89.

we have $P = 30$ dBm and $P_0 = -50$ dBm, hence the signal power decay is reasonable. By (10) with $\tau_0 = 4$, we have $\bar{\alpha} \approx 4.0$. In simulations, we only consider the interference-limited networks, i.e., the noise power is assumed to be 0.

A. Cell Shape: Irregular Shape vs. Disk

Fig. 3 compares the coverage probability for the JSP model with irregular cell shapes and disk approximation of the cell shape given different values of (λ, P_0), where $\bar{\alpha}$ is given in (10). The disk approximation of the cell shape is quite accurate, especially in the high-reliability regime, i.e., when θ is small, for all values of (λ, P_0) that we choose. Consider the parameter setting Case 1 with $(\lambda, P_0) = (3.5\times10^{-5}, 1\times10^{-8})$ as a reference. Case 3 with $(\lambda, P_0) = (1 \times 10^{-4}, 1 \times 10^{-8})$ has better coverage probability, while Case 2 with $(\lambda, P_0) = (3.5 \times 10^{-5}, 1 \times 10^{-7})$ has worse coverage probability. One dominating reason is the difference of $\bar{\alpha}$. For example, compared to Case 1, Case 2 has a larger P_0 and a larger desired received signal power averaged over the fading. Case 2 should have a better coverage than Case 1, if the interference levels (indicated by $\bar{\alpha}$) were the same. But in fact, the interference in Case 2 is much higher and Case 2 has a worse coverage, as is shown in Fig. 3, which implies that $\bar{\alpha}$ is a dominating factor.

B. Distribution of the Local Path Loss Exponent

In Fig. 4, the empirical PDF of the local path loss exponent for the desired received signal the JSP model with irregular cell shapes is drawn. We choose the known probability distributions—the gamma distribution and the inverse gamma distribution and use the maximum likelihood estimation (MLE) method to approximate the empirical PDF. For the gamma distribution, the PDF is expressed as $f_{\rm gamma}(x) = x^{k-1}\exp(-x/a)/(a^k\Gamma(k))$, the mean is ka and the variance is ka^2. For the inverse gamma distribution, the PDF is expressed as $f_{\rm igamma}(x) = a^{\kappa-1}x^{-\kappa-1}\exp(-a/x)/\Gamma(\kappa)$, the mean is $a/(\kappa-1)$ and the variance is $a^2/((\kappa-1)^2(\kappa-2))$. Fig. 4 shows that both fits provide good matches with the inverse gamma distribution fit slightly better than the gamma distribution fit. We observe that most empirical local path loss exponents falls in the range $[3.5, 4.5]$; outside the range, according to the fitting results, the PDF decays fast.

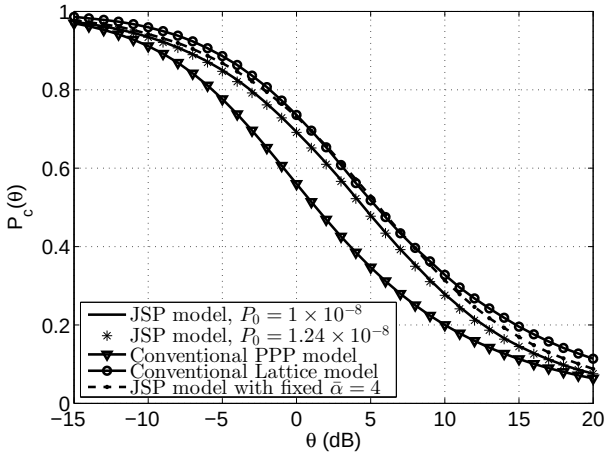

Fig. 5. Comparison between the JSP models with irregular cell shapes ($(P_0, \lambda, \bar{\alpha}) = (1\times10^{-8}, 3.5\times10^{-5}, 4.0), (1.24\times10^{-8}, 3.5\times10^{-5}, 3.95)$) and conventional models—the conventional PPP model and the conventional triangular lattice model ($\lambda = 3.5 \times 10^{-5}$ and $\alpha = 4.0$). For the JSP model with fixed $\bar{\alpha} = 4$ (the dashed line), $P_0 = 1.24 \times 10^{-8}$, $\lambda = 3.5 \times 10^{-5}$ and $\bar{\alpha}$ is not given in (10), but is a constant 4.

C. JSP Model and Conventional Model

Since the JSP model is brand new, it is crucial to compare our model with the conventional model to see how different our model performs. We use the simulation result of the JSP model with irregular shapes to do the comparison, not the approximation result (i.e., the JSP model with disk approxima-

tion of the cell), although our approximation provides accurate coverage probability in the high-reliability regime. Consider the JSP model with irregular cell shapes ($\lambda = 3.5 \times 10^{-5}$, $P_0 = 1 \times 10^{-8}$ and by (10), $\bar{\alpha} = 4.0$). We assume a path loss exponent $\alpha = 4$ and the same intensity $\lambda = 3.5 \times 10^{-5}$ for the conventional model. Fig. 5 compares the JSP model with irregular cell shapes and two conventional models—the conventional PPP model and the conventional triangular lattice model. Note that in the conventional PPP model [1], $P_{\mathrm{c}}(\theta) = (1 + \sqrt{\theta}\arctan(\sqrt{\theta}))^{-1}$. It has been shown that in conventional models, the coverage curve of a general point process is quite accurately approximated by a horizontal shift (gain) of the curve of the PPP [3], [6]. The triangular lattice has the largest gain of 3.4 dB.

We observe that the coverage probability of the JSP model lies between that of the two conventional models and is close to that of the conventional triangular lattice model. The actual network perceived by the typical user is approximately a conventional triangular lattice network. The small gap (roughly 1 dB horizontal difference) between the JSP model and the conventional lattice model mainly results from the fact that the received signal powers averaged over the fading at the cell edges are not equal for the two models. If we approximate the hexagonal cell shape as a disk, we can obtain the received power at cell edges, which is 1.24×10^{-8} and is larger than 1×10^{-8}.

Consider the JSP model with $\lambda = 3.5 \times 10^{-5}$ and $P_0 = 1.24 \times 10^{-8}$. By (10), $\bar{\alpha} = 3.95$. We observe in Fig. 5 that this JSP model has the same performance as the JSP model with $\lambda = 3.5 \times 10^{-5}$ and $P_0 = 1 \times 10^{-8}$. There is a roughly 1 dB horizontal gap between the JSP model and the conventional lattice model. It is mainly because the interference level in the JSP model is higher than that in the conventional lattice model, since $\bar{\alpha} < 4.0$.

To investigate how much impact the path loss exponent $\bar{\alpha}$ for the interference has on the coverage probability in the JSP model, we here assume $\bar{\alpha}$ is not given in (10), but is a constant 4.0 for the JSP model with $\lambda = 3.5 \times 10^{-5}$ and $P_0 = 1.24 \times 10^{-8}$. As is shown in Fig. 5, the new case nearly overlaps with that of the conventional lattice model. Therefore, the difference in $\bar{\alpha}$ is the main reason of the 1 dB gap between the JSP model and the conventional lattice model.

V. Conclusions

In this paper, we argue that a new class of models is needed—the joint spatial and propagation models, where BSs are deployed to make all users at cell edges achieve a minimum target signal power level from the serving BS. In other words, the BSs are deployed "optimally" given the surrounding signal propagation conditions. We proposed an instance of such a JSP model, where the target signal power on the cell edges is achieved using a variable path loss exponent. Then, for networks where the BSs form a homogeneous PPP, we obtained the expressions of the coverage probability by approximating the irregular Voronoi cell shapes as disks of the same cell size. Simulation results showed that the approximation is quite accurate.

It is insightful to contrast our results with those in [5], where it is proved that with increasing shadowing variance, the received powers at the origin for all motion invariant point processes and lattices converge weakly to those of a PPP, which means that the actual network is perceived by a typical user as an equivalent Poisson point process distributed network, provided shadowing is strong enough.

Our results show that the JSP model exhibits a coverage performance that is very similar to that of a triangular lattice. Hence we come to the opposite conclusion of [5], which stated that *wireless networks appear Poissonian due to strong shadowing*. Here we have demonstrated that *Poisson networks appear like lattices due to dependence between propagation and BS placement*. This shows that even though BSs may geographically form a PPP, the resulting performance is not as bad as previously assumed if the dependence between cell sizes and propagation conditions is accounted for.

Acknowledgment

The partial support of the U.S. National Science Foundation through grants CCF 1216407 and CCF 1525904 is gratefully acknowledged.

References

[1] J. G. Andrews, F. Baccelli, and R. K. Ganti, "A tractable approach to coverage and rate in cellular networks," *IEEE Transactions on Communications*, vol. 59, no. 11, pp. 3122–3134, Nov. 2011.

[2] N. Deng, W. Zhou, and M. Haenggi, "The Ginibre point process as a model for wireless networks with repulsion," *IEEE Transactions on Wireless Communications*, vol. 14, no. 1, pp. 107–121, Jan. 2015.

[3] A. Guo and M. Haenggi, "Asymptotic deployment gain: A simple approach to characterize the SINR distribution in general cellular networks," *IEEE Transactions on Communications*, vol. 63, no. 3, pp. 962–976, Mar. 2015.

[4] ——, "Spatial stochastic models and metrics for the structure of base stations in cellular networks," *IEEE Transactions on Wireless Communications*, vol. 12, no. 11, pp. 5800–5812, Nov. 2013.

[5] B. Blaszczyszyn, M. Karray, and H. Keeler, "Wireless networks appear Poissonian due to strong shadowing," *IEEE Transactions on Wireless Communications*, vol. 14, no. 8, pp. 4379–4390, Aug. 2015.

[6] M. Haenggi, "The mean interference-to-signal ratio and its key role in cellular and amorphous networks," *Wireless Communications Letters, IEEE*, vol. 3, no. 6, pp. 597–600, Dec 2014.

[7] P. Calka and T. Schreiber, "Limit theorems for the typical Poisson-Voronoi cell and the Crofton cell with a large inradius," *The Annals of Probability*, vol. 33, no. 4, pp. 1625–1642, Jul. 2005.

[8] J.-S. Ferenc and Z. Neda, "On the size distribution of Poisson-Voronoi cells," *Physica A-Statistical Mechanics And Its Applications*, vol. 385, no. 2, pp. 518–526, 2007.

[9] J. Mecke, "On the relationship between the 0-cell and the typical cell of a stationary random tessellation," *Pattern Recognition*, vol. 32, no. 9, pp. 1645–1648, 1999.